ADVANCED MATERIALS

Supporting Information

for *Adv. Mater.*, DOI: 10.1002/adma.202002127

Ultralong-Range Energy Transport in a Disordered Organic Semiconductor at Room Temperature Via Coherent Exciton-Polariton Propagation

*Shaocong Hou, Mandeep Khatoniar, Kan Ding, Yue Qu, Alexander Napolov, Vinod M. Menon, and Stephen R. Forrest**

Supporting Information

Ultralong-range energy transport in a disordered organic semiconductor at room temperature via coherent exciton-polariton propagation

Shaocong Hou, Mandeep Khatoniar, Kan Ding, Yue Qu, Alexander Napolov, Vinod M. Menon, Stephen R. Forrest[*]

Figure S1. Atomic Force Microscope (AFM) images of (a) DBR and (b) 20 nm DBP film on DBR showing a typical flat surface morphology of amorphous organic film.

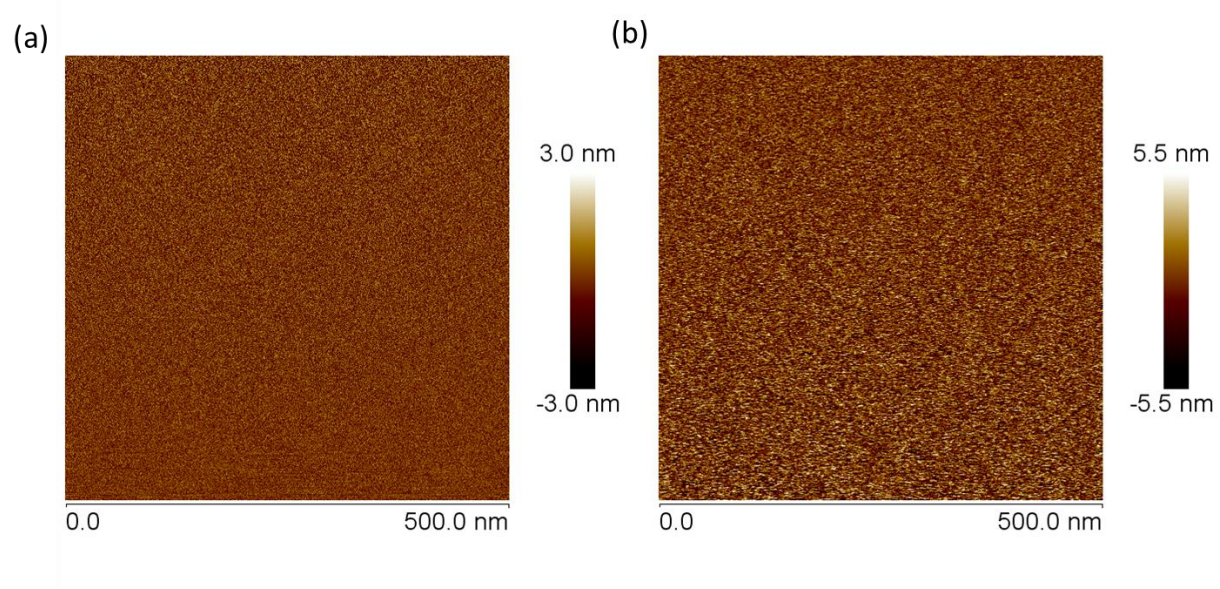

Figure S2. X-ray diffraction of fused silica substrate (black line), 20 nm DBP film on a fused silica substrate and 40 nm DBP film on a fused silica substrate ((blue line). No organic crystalline peak was detected confirming an amorphous structure of DBP film. This finding is consistent with a previous report [1].

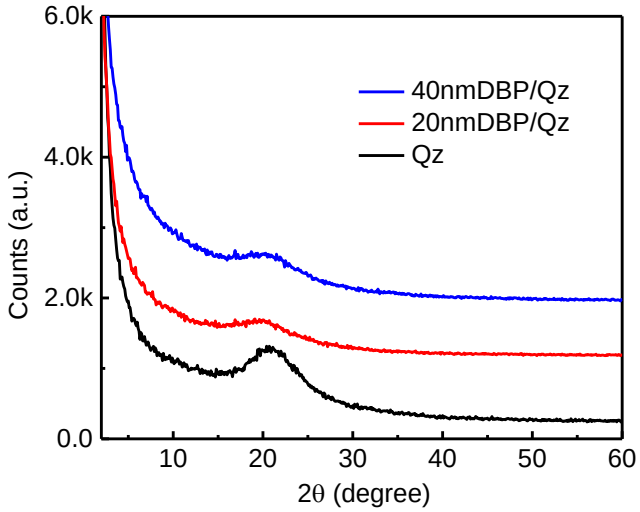

Figure S3. The k-space PL microscope setup for k-space filtering (upper detection channel) and real-space filtering measurements (lower detection channel).

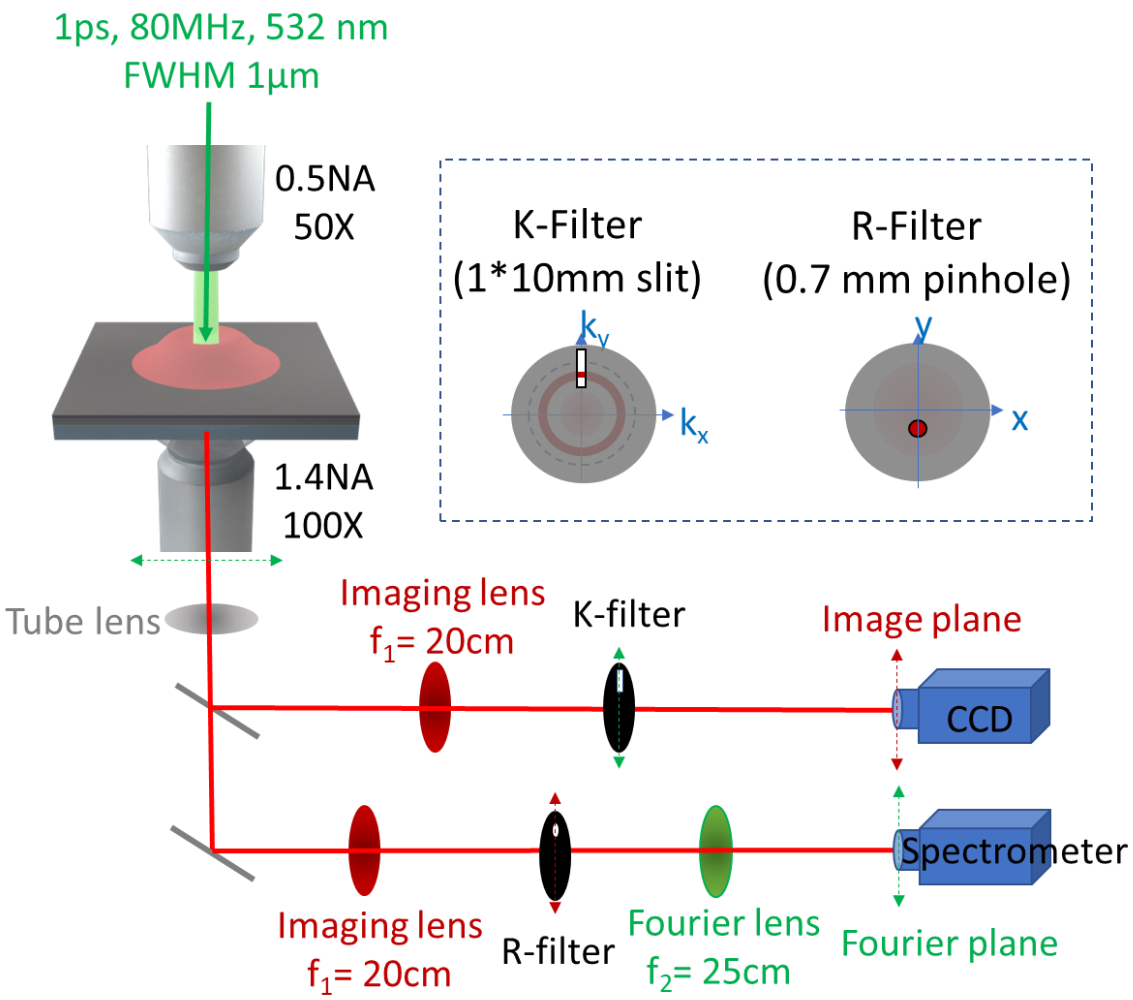

The angular reflectivity was measured using a *k*-space microscope comprising an inverted microscope (Olympus), a white tungsten halogen white lamp source, and a spectrometer (Acton SpectraPro SP-2500) with a 1024 x 1024 CCD camera (PIX 1024B, Princeton Instruments). The measurement was conducted in a reflection geometry with a 1.40 NA, 100x oil-immersed objective. The *k*-space image was reconstructed at the entrance of the spectrometer using an achromatic lens (Thorlabs), and the reflected light is filtered by a linear TE polarizer. The angular photoluminescence spectra were collected with a similar microscope setup using a

TM-polarized λ = 532 nm ultrafast pulsed laser source (pulse width of 1 ps, repetition time of 80 MHz, power of 1 μW; Toptica Fibre-Pro) and a λ = 600 nm long pass filter (Thorlabs) to remove the pump radiation from the light collection path.

Photoluminescence images were collected by the k-space microscope in a transmission geometry using the set-up in Fig. S3 (Supplementary Information). A 1 μm diameter TE-polarized pulsed Gaussian laser beam was focused on the surface of the DBP layer with a 0.5NA, 50x objective. Direct coupling of the pumping light into the surface modes of the sample is avoided. Emission was collected as above. In the collection channel for k-space-filtered real space imaging, a 5 cm diameter achromatic lens was used to reconstruct the real-space image at the entrance of a CCD camera. A 1 mm x 10 mm slit was placed in the reconstructed *k*-plane after the lens and moved by a micromanipulator to admit only the emission light with the desired *k*. The position of the slit was confirmed by a flip lens. For wavelength-resolved propagation measurements, the CCD camera was replaced with a spectrometer. The position of the slit filter has a significant effect on the propagation pattern. The edge of the slit may diffract the exiting light, resulting in an additional shift of the propagation pattern as well as the generation of optical fringes. To minimize edge diffraction, the slit edge was placed slightly below the air cone where there was only negligible exciton emission. In the collection channel for real-space-filtered *k*-space photoluminescence imaging (bottom chanel in Fig. S3), the image was reconstructed by a 5 cm diameter achromatic lens. A 500 μm pinhole was used to select a particular area, and its position in the image plane was confirmed by a flip lens. The filtered light passed through a second 5 cm diameter achromatic lens and projected onto the spectrometer at the k-plane.

Figure S4. The k-space PL image before (a) and after (b) put on a k-space filter.

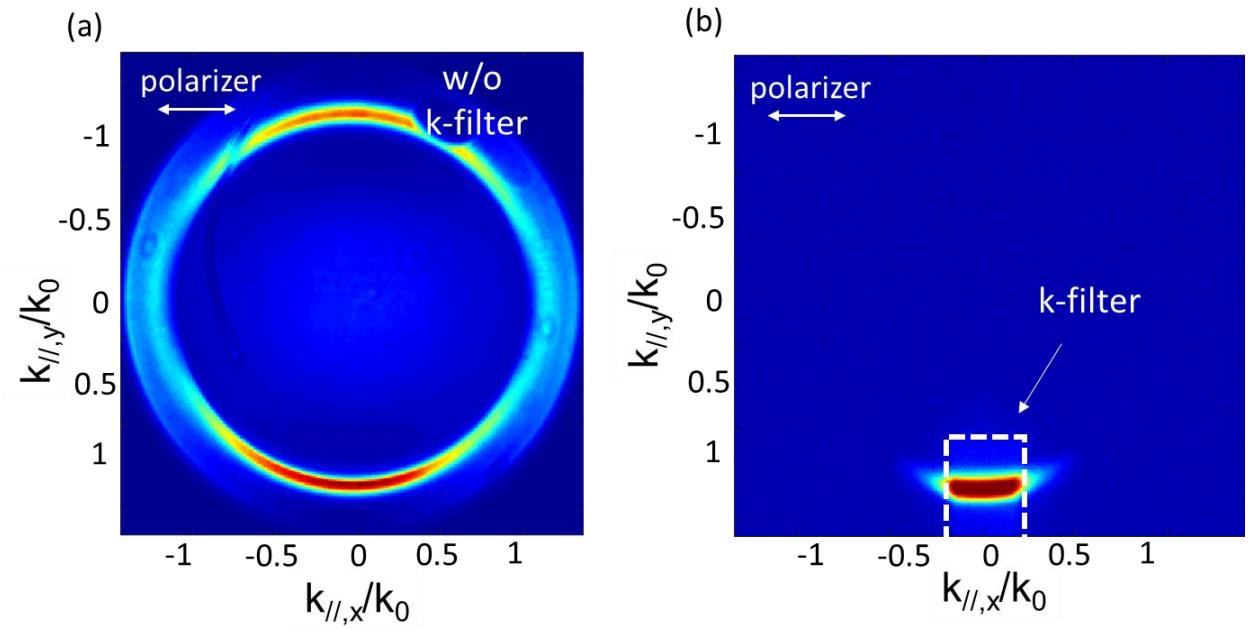

Figure S5. (a) PL spectra at momentum *k* (solid line) or -*k* (dashed line), and pinhole position of 0 μm (back line) or 17 μm (red line) obtained from Fig. 3. (b) PL spectra at the same *k* blueshift when moving the spatial pinhole filter to a position at a distance of 0, 10, 17, and then back to near 0 μm from the pumping center. PL peak position (c) and full width at half maxima (d) derived from (b). Data point derived from the spectra back to near 0 μm is shown in red.

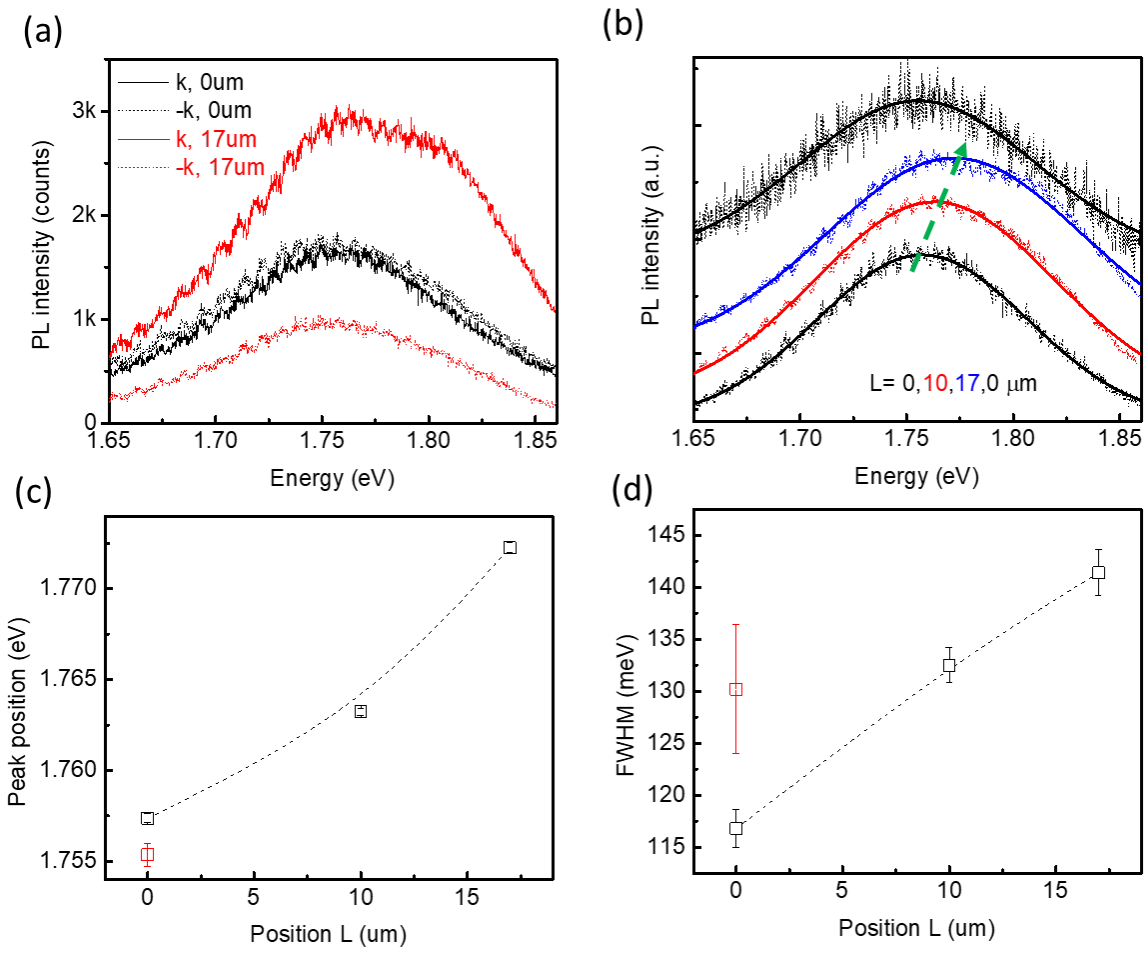

Figure S6. PL image showing polariton propagation in the absence of a *k*-space filter. Emission from the TE and TM modes is separated using a linear polarizer. The horizontal dashed-line indicates propagation of TM guided modes, while the vertical dashed-line indicates the propagation direction of TE polaritons. The excitation laser beam is focused at position (0, 0), showing an intense peak from leakage of exciton emission.

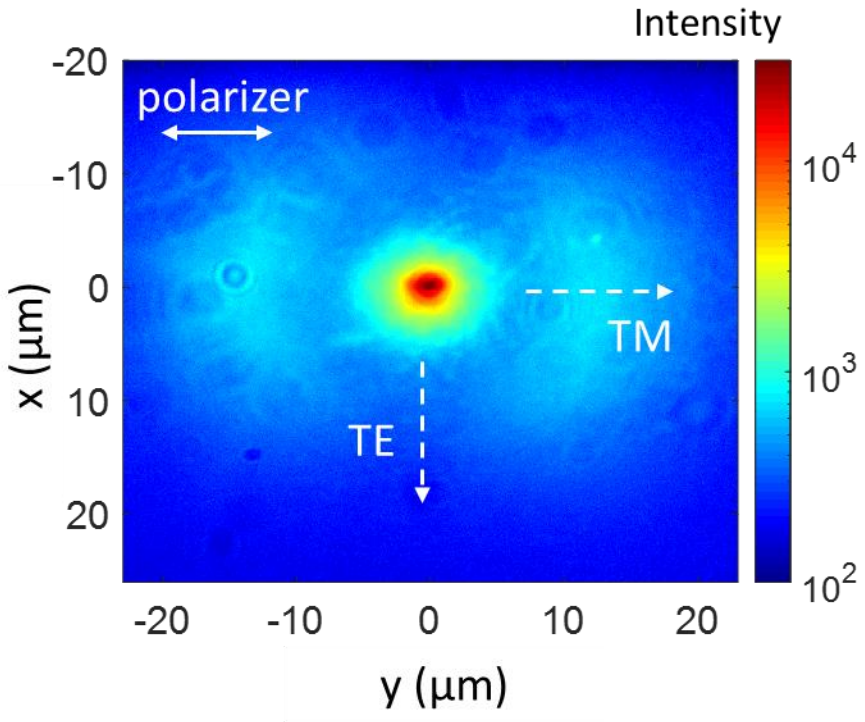

Figure S7. PL spectra of the control sample with 20 nm DBP on silica. (a) Measured TE angular PL spectra showing significant emission weakly coupled into the substrate mode. (b) Energy-resolved PL image after filtering the low-*k* emission within the air cone, showing a hole pattern centered at the pumping position x = 0 μm. Note that the right edge in (a) and vertical cut-line in (b) are measurement artifacts.

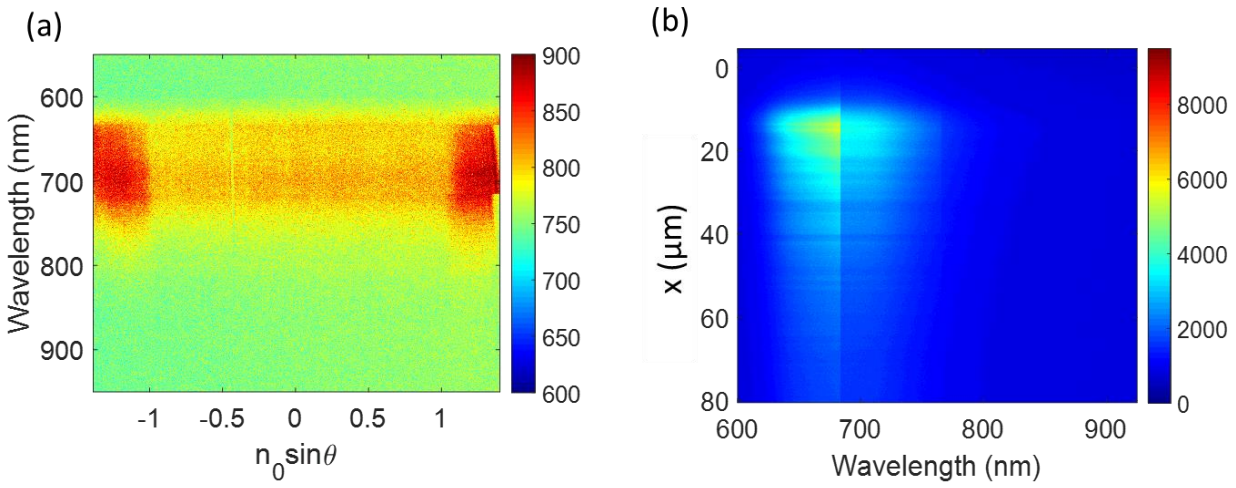

Figure S8. (a) PL spectra at different nonresonant pumping powers from 0.4 μW to 1.58 mW. (b) PL peak position derived from (a) shows an energy blueshift.

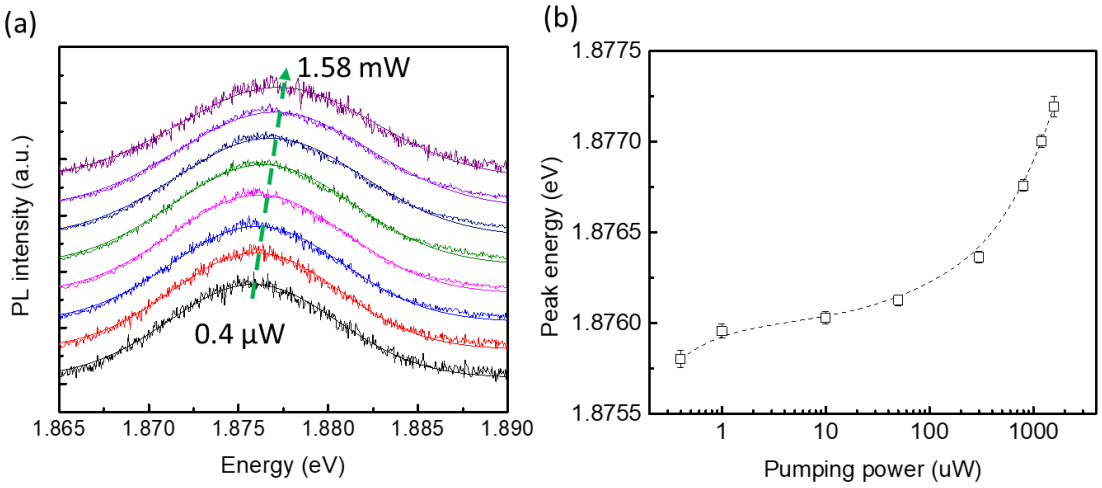

Figure S9. Schematic structure of the polariton device

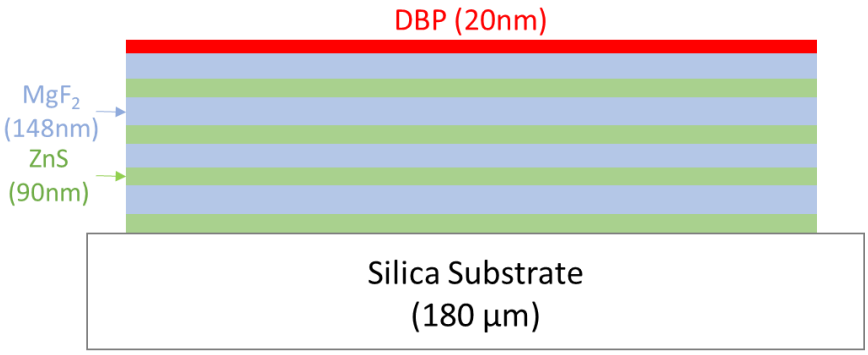

Figure S10. Polariton propagation profiles at wavelengths of 690, 710, 730 and 750 nm. Note than the edge position of *k*-slit filter is slightly shifted towards higher-*k* side compared with that in Figure 2 and Figure 4.

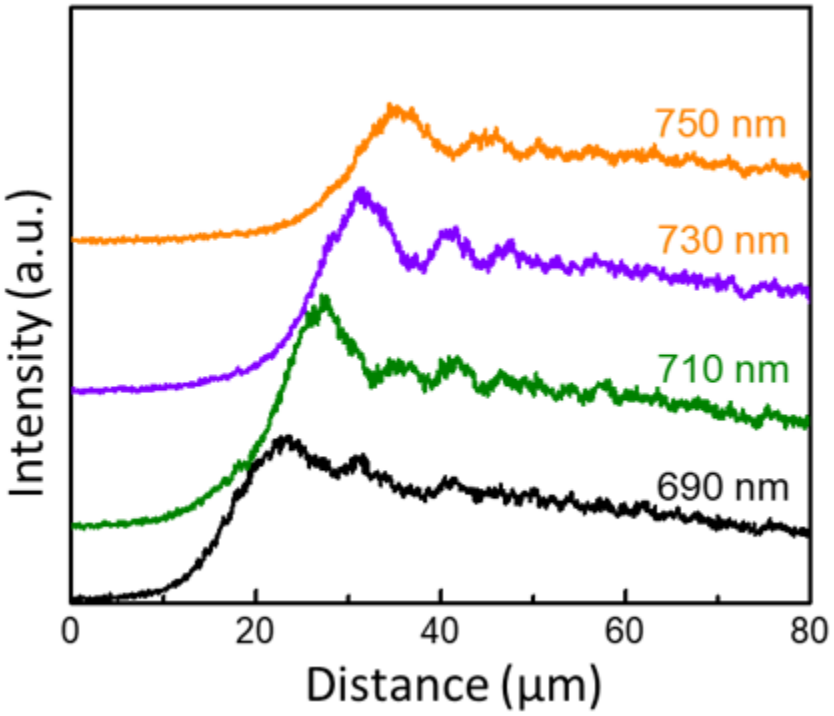

Self-Interference Model

The polariton propagation pattern is due to self-interference of modes as illustrated in Fig. 4b. Consider two plane wave components emitted from a DBP exciton whose transition dipole moment is oriented parallel to the substrate plane. The propagation proceeds at angle, θ (path 1), and -θ (path 2). When (π - θ) is larger than the critical angle between DBP and air (θ_c), path 2 experiences TIR at the top DBP surface, resulting in a phase difference between paths 1 and 2. The phase difference φ is given by:

$$\varphi = \arctan\left(\frac{\sqrt{\cos^2\theta - \left(\frac{n_{\text{air}}}{n_{\text{DBP}}}\right)^2}}{\sin\theta}\right) + \frac{4\pi z n_{\text{DBP}}}{\lambda\cos\theta}, \qquad (1)$$

where n_{air} and n_{DBP} are the refractive indexes of air and DBP respectively, λ is the wavelength of the exciton radiation, z is the distance of the exciton to the DBP top surface. The first term is the phase delay due to TIR, whereas the second term is the phase delay due to the additional length of path 2.

The Fourier transform of the electric field $E(\vec{r})$ radiated by the DBP exciton is:

$$E(\vec{r}) = \int E(\vec{k}) e^{-i\vec{k}\cdot\vec{r}} d\vec{k} = \int_{-\frac{\pi}{2}+\theta_c}^{\frac{\pi}{2}-\theta_c} E(\theta)\, e^{-ik(cos(\theta)x + \sin(\theta)z)} d\theta$$

$$= \int_{0}^{\frac{\pi}{2}-\theta_c} \left(E(\theta)\, e^{-i(k_x\cdot x + k_z\cdot z)} + E(-\theta) e^{-i(k_x\cdot x - k_z\cdot z)}\right) d\theta, \qquad (2)$$

where $\vec{r}$ is the position vector within the DBP film, x is in-plane component of $\vec{r}$, k_x and k_z are the in-plane and out-of-plane components of the wavevector $\vec{k}$, respectively, and $E(\theta)$ and $E(-\theta)$ are the electric fields of the plane waves along path 1 and path 2, respectively.

Following reflection, path 2 has the identical wavevector as path 1, thus the same coupling efficiencies to the polariton mode. Consequently, the amplitudes of the two plane waves are also the same, viz. $E(\theta) = E(-\theta)$. The two plane waves each excite a polariton component with the electric field, $E_{\mathrm{LP}}(x)$, that is calculated by summing the polariton mode excited by all plane wave components in (2):

$$E_{\mathrm{LP}}(x) = \int_0^{\frac{\pi}{2}-\theta_c} (E_{\mathrm{LP}}(\theta)\, e^{-ik_{x1}\cdot x} + E_{\mathrm{LP}}(\theta) e^{-i(k_{x2}\cdot x+\varphi)}) d\theta, \qquad (3)$$

where $E_{\mathrm{LP}}(\theta)$ is the electric field amplitudes of polariton modes excited by plane wave, $E(\theta)$, and k_{x1} and k_{x2} are in-plane wavevector components of the polariton excited via path 1 and path 2, respectively.

We assume that $k_{x1,0} = k_{x2,0} = k_{x,0}$ at the excitation spot at $x = 0$. After propagation over a distance x, k_{x1} and k_{x2} scatter into Gaussian distributions with standard deviation $\sigma = \mu x$, where μ is the broadening factor. Polariton modes following these two paths that are excited by the same exciton interfere with each other. Thus, the total intensity of polariton emission is given by:

$$I_{\mathrm{LP}}(x) = \int_0^d \left(\int_0^{\frac{\pi}{2}-\theta_c} E_{\mathrm{LP}}(\theta) e^{-ik_{x1}\cdot x} (1 + e^{-i\Delta k_x \cdot x}\, e^{-i\varphi}) d\theta \right)^2 e^{-\alpha x} dz, \qquad (4)$$

where $\Delta k_x = k_{x2} - k_{x1}$, α is the attenuation due to leakage and absorption during propagation, z is the distance from the DBP free surface, and d is the film thickness. When the polariton mode propagates to x, the phase decoherence $\Delta\varphi$ accumulates as:

$$\Delta\varphi = \int_0^x \sigma dx = \frac{\mu x^2}{2}, \quad (5)$$

The coherence length, l_{coh}, is the distance where $\Delta\varphi$ reaches 2π, i.e. $l_{coh} = \sqrt{\frac{4\pi}{\mu}}$.

The polariton propagation pattern for a given wavelength is calculated by choosing the polariton components for k_x in the integral of Eq. (4). The fitting parameters μ and α used in the fit to the experimental data in Fig. 4c are listed in Table S1. The total propagation length is defined as $L_{1/e} = L_{hole} + L_{decay}$, where the hole size, L_{hole}, is the distance from the pumping location to the PL intensity peak, and the decay length, L_{decay}, is the distance where the peak intensity has decreased by a factor of 1/e from the intensity maximum, that is, $L_{decay} = 1/\alpha$.

Following ref. 13, the phase-breaking length l_{inel} due to inelastic polariton scattering is $l_{inel} = v_g \tau_{pol}$, where v_g is group velocity of the LP polariton. The LP polariton lifetime is $\tau_{pol} = (\frac{C_{ex}^2}{\tau_{ex}} + \frac{c_{BSW}^2}{\tau_{BSW}})^{-1}$, where C_{ex}^2 and C_{BSW}^2 are excitonic and photonic weights of the polariton, respectively, and τ_{ex} and τ_{BSW} are lifetimes of the uncoupled exciton and BSW photon.

Table S1. Parameters of the interference model to fit the propagation profiles in Fig. 4c.

Wavelength (nm)	670	690	710	730	750
μ (μm^{-2})	0.014	0.032	0.045	0.059	0.073
α (μm^{-1})	0.039	0.016	0.013	0.01	0.009

Reference

[1] S Grob, et al. J. Mater. Chem. A **2015**, 3, 15700